Mast cell changes the phenotype of microglia via histamine

Maria Pilar Ramirez-Ponce
Universidad de Sevilla Facultad de Medicina
Alejandro Sola-Garcia
Universidad de Sevilla Facultad de Medicina
Santiago Balseiro-Gomez
Yale University School of Medicine
Maria Dolores Maldonado
Universidad de Sevilla Facultad de Medicina
Jorge Acosta
Universidad de Sevilla Facultad de Medicina
Eva Ales (eales@us.es)
Universidad de Sevilla Facultad de Medicina https://orcid.org/0000-0002-5536-4616
Juan Antonio Flores
Universidad de Sevilla Facultad de Medicina

Research

Keywords: Ca2+ imaging, exocytosis, phagocytosis, histamine, ATP, mast cells, microglia

Posted Date: November 19th, 2019

DOI: https://doi.org/10.21203/rs.2.17388/v1

Abstract

Background Microglia are the dynamic, motile phagocytes of the brain considered the first line of defense against threats or disturbances to the Central Nervous System (CNS). Microglia help orchestrate the immunological response by interacting with immune cells. Mast cells (MCs) are effector cells of the innate immune system distributed in all organs and vascularized tissues, brain included. Several molecular mechanisms for potential interactions between MCs and microglia have been determined. However, the effect of MCs on regulated exocytosis and phagocytic clearance in microglia has not been explored.

Methods Cocktails of MCs mediators (MCM) obtained at 37ºC and 53ºC were used to induce microglia activation. Changes in intracellular calcium [Ca2+]i and ATP release were studied by calcium and quinacrine fluorescence imaging. Fluorescent latex beads were used to assay phagocytosis in microglia after MCM treatment and compared to that measured in the presence of histamine, ATP and lipopolysaccharide (LPS). Iba-1 expression was quantified by immunofluorescence and histamine levels evaluated by ELISA measurements.

Results Local application onto microglia of the MC mediator cocktail elicited Ca2+ transients and exocytotic release associated with quinacrine dye de-staining. Ca2+ signals were mimicked by histamine and blocked by the H1 receptor (H1R), cetirizine. However, hydrolysis of ATP, by apyrase also affected Ca2+ transients to a lesser extent. Phagocytosis was enhanced or inhibited by MCM depending on the histamine concentration. Low levels of histamine increased iba-1 fluorescence and a number of internalized microbeads per cell whereas high levels prevented iba-1 expression and microglial phagocytosis.

Conclusions Our results highlight the relevance of MC-derived histamine in the modulation of secretory and phagocytic activities that ultimately may explain the heterogeneity of microglial responses in different pathological contexts and why microglia can be either neuroprotective or neurotoxic, resulting in confinement or aggravation of disease progression.

Background

Chronic inflammation in CNS is a hallmark of neurodegenerative disorders in which progressive loss of neurons and altered physicochemical properties in the brain are observed [1][2].Microglia cells, key players in such disorders, are the resident phagocytes of the brain and play an important role in maintaining normal brain function. Pathological states within the nervous system can lead to microglial activation, characterized by morphological changes, proliferation, and migration towards the injury site; phagocytosis; and secretion of various cytokines, chemokines, and other inflammatory mediators [3]. Activation of microglial cells can result in different phenotypes and roles (neurotoxic or neuroprotector) with versatile actions and variable responses depending on the stimulus intensity and context [4].

In their resting state, microglial cells display a ramified morphology characterized by numerous, fine-branched processes with relatively small bodies. When activated in response to injury or inflammatory stimuli, the resting microglia increase Ca^{2+} permeability that leads to Ca^{2+} influx into the cells. This increase of intracellular calcium $[Ca^{2+}]_i$ acts as a versatile intracellular second messenger that initiates signaling cascades, leading to essential biological processes such as the morphological transformation [5] in which cells become progressively less ramified and quickly develop an ameboid appearance with an enlarged cell body and several short, thickened processes. Elevations of $[Ca^{2+}]_i$ in microglial cells is also required in ATP and BDNF secretion through Ca^{2+} dependent exocytosis from lysosomes and secretory granules [6][7]. Given the involvement of lysosomal secretion in cytokine release [8][9], the exocytotic process can be crucial to define the phenotype acquired by these plastic cells upon activation. In addition, microglial functions such as motility and phagocytosis are closely associated with dynamic changes in the cytoskeleton and related to intracellular calcium signaling [10][11].

Microglia can respond to pro-inflammatory signals released from other non-neuronal cells of immune origin, which includes mast cells (MCs). These cells reside in the brain and can traverse the blood-brain barrier in healthy and pathological conditions [12][13]. MCs contain numerous secretory granules that hold a wide spectrum of mediators, including biogenic amines such as histamine and serotonin, enzymes, ATP, neuropeptides and proteogycans [14]. In addition to rapid mediator release of preformed granule constituents via degranulation, longer-term activation results in the release of the *novo* formed mediators such as lipid mediators and cytokines [15]. Brain MCs are activated in CNS disorders and induce the release of several mediators. MCs were reported to induce microglial activation and inflammatory mediator release [16][17] suggesting a pivotal role of these cells in the induction of CNS inflammation. Thus, the suppression or stabilization of brain MCs degranulation can inhibit both microglial activation and CNS inflammation [18][19][20].

Mast cell-microglia communication contributes to accelerate disease progression. However, the functional consequences of MCs in microglial exocytosis and phagocytosis remain unexplored. Microglia activation is associated to secretion of several molecules, which either propagate inflammation and cause damage to neurons or play a neuroprotective role [21]. Microglia phagocytises foreign pathogens, apoptotic cells, myelin debris and released toxic proteins. In this study, In this study, we imaged changes in $[Ca^{2+}]_i$ and, measured exocytosis of ATP-containing vesicles and the phagocytic activity of microglia evoked by a cocktail of MCs mediators. Our results suggest MC may trigger two distinct functional microglial responses, which could exacerbate damage or protect.

Methods

Cocktail of mast cells mediators

A cocktail of mast cells mediators (Mast cells Conditioned Medium, MCM) was prepared as previously described [22]. Briefly, 1 x 10^6 purified MCs obtained after a 70% Percoll purification were resuspended in

1 ml of basal Locke solution containing 140 mM NaCl, 10 mM HEPES, 3 mM KOH, 2 mM $CaCl_2$, 1 mM $MgCl_2$, and 10 mM glucose (pH 7.3, adjusted with NaOH). Cells were placed into a prewarmed Thermomixer (Eppendorf) for 1h at 53ºC with moderate agitation (600 rpm). MC degranulation was verified by visual inspection under a microscope. The MCM was obtained from the supernatant after centrifugation of MCs solution at 200xg for 5 min. Supernatant was aliquoted (50 µl) and stored at −80 °C until use. MCM from MCs kept at 37ºC, 5% $C0_2$ for 1 h was obtained to evaluate the degree of degranulation in basal conditions.

Enzyme-Linked Immuno-Sorbent Assay (ELISA)

The expression of histamine levels in MCM was quantified with a commercial ELISA kit from Beckman Coulter (IMMUNOTECH—Prague, Czech Republic) following the manufacturer's instructions. All samples were run in duplicate.

Microglia-Enriched Cultures

Isolated microglia were obtained using a mild trypsinization over mixed glial cultures as previously described [23] with slight modifications.

Mixed glial cultures were prepared from cerebral cortices of postnatal (P2-P4) Wistar rats, which were subjected to mechanical dissociation. After filtering cells through a filter nylon mesh of 100 µm, the cells obtained were seeded in Dulbecco's modified Eagle's medium (DMEM)/F12 with 20% of inactivated foetal bovine serum (FBS) at a density of 300,000 cells/ml on 15 mm-diameter cover glass and maintained at 37ºC in a humidified atmosphere of 5% CO_2/95% air. Culture medium was replaced after 5 days *in vitro* (DMEM/F12 and 10% of inactivated FBS). After reaching a confluent monolayer of glial cells (10–12 days), microglia-enriched cultures were obtained with a trypsin solution (0,05% trypsin and EDTA) diluted 1:4 in DMEM/F12. This process resulted in the detachment of the upper layer of cells in one piece, while microglial cells remained attached on the surface of the cover glass. Mild trypsinization has been proved to be a reliable method to isolate microglia from mixed glial cultures with increased yield and purity and microglial cells seem to be in an immune state closer to their resting state in comparison with the shaking method [24]. However, our cultures did not exceed 15% of cells with a resting phenotype.

Recordings of $[Ca^{2+}]_i$ signal

Changes in $[Ca^{2+}]_i$ of microglial cells in response to different stimuli were monitored by dual excitation microfluorimetry. Microglial cells were incubated in Locke external solution containing Fura–2 AM 5 µM (Molecular Probes) and pluronic F–127 0.004%, (Sigma) for 45 min at 37ºC in the dark. Later, cells were washed twice in external solution without the dye and used for imaging. The cover glass with cells loaded with Fura–2 AM was then mounted in a RC–25F perfusion chamber (Warner instruments) and placed on

the microscope (AxioVert 200, Zeiss). During recordings, microglial cells were excited by a xenon light source at 360/380-nm wavelengths (exposure time, 0.5 s; data acquisition at 0.33 Hz) by means of two narrow beam band-pass filters selected by a computer-controlled wheel. The emitted fluorescence was filtered through a 520-nm filter and captured with an ORCA-R2 CCD camera (Hamamatsu Photonics). Fura–2 AM loading was usually uniform over the cytoplasm, and dye compartmentalization was never observed. Data were acquired and stored using HCImage software and exported to Igor Pro (WaveMetrics) to perform analysis. All values were normalized to the basal fluorescence (baseline). The $[Ca^{2+}]_i$ signal was expressed by the ratio of fluorescence at 360 nm and 380 nm. The agents used to stimulate microglia were MCM, histamine 100 μM, serotonin 100 μM and ATP 100 μM. When required, cells were incubated with cetirizine 1 μM or FSLLRY-NH2 (PAR2 antagonist) 400 μM for 10 min at 37ºC before the application of MCM or histamine. MCM was treated with apyrase 50 U/ml for 10 min, chondroitinase ABC 50 mU/ml or heparinase 0.5 U/ml for 1 h at 37ºC to evaluate the effect of ATP, chondroitin sulphate or heparin from the MCM on microglial cells, respectively. These products were applied through a pressure pulse (5 s) with a micropipette (1 μm diameter) positioned approximately 100 μm to the microglial cell. All experiments were performed at 37 °C.

Imaging and analysis of Quinacrine dye release

To visualize microglial acidic organelles, microglia was treated with 10 μM quinacrine in Locke external solution for 10 min at 37ºC in the dark. Later, microglial cells were washed twice in external solution without the dye and used for imaging. The cover glass with cells loaded with quinacrine was then mounted and transfer to the chamber for imaging under an inverted microscope with a 63× PlanNeofluar (NA 1.3) oil immersion lens (Zeiss). The fluorescence images were collected every 5s, with excitation at 472 nm and emission at 579 nm. Data analysis was performed with HCImage software (Hamamatsu). Time-lapse imaging of quinacrine fluorescence was evaluated after application of MCM, histamine 100 μM, ATP 100 μM and LPS 1 μg/ml.

Phagocytosis Assay and Microglia Immunofluorescence

After mixed glia culture was subjected to trypsin treatment, microglial cells were allowed to recover for 24h, after which the cells were ready to undergo some microglial treatments for 6h and 48h. These treatments were as follows: control (without any treatment), 10% MCM, 1μg/ml of LPS, 10 μM histamine, 100 μM histamine and 100 μM ATP. Later we proceeded to the phagocytosis assay (blind experiments). This is as follows (with some modifications [25]). Fluorescent latex beads were used to assay phagocytosis. Fluorescent beads were pre-opsonized in non-inactivated FBS for 1h at 37ºC. Ratio of beads to FBS was 1:5. Beads-containing FBS with DMEM/F12 with 10% of inactivated FBS were diluted to reach final concentrations for beads and FBS in DMEM/F12 of 0.01% (v/v) and 0.05% (v/v), respectively. Then, cell cultures were incubated with beads-containing medium at 37ºC for 1h and washed thoroughly with ice-cold PBS 5 times. Next, cells were fixed using 4% PFA for 30 min at room

temperature. After that, we performed iba–1 immunofluorescence. Firstly, cells were permeabilized with 0.1% Triton X–100 in PBS and, after adding blocking solutions for 1h at room temperature, incubated overnight with rabbit anti-Iba1 monoclonal antibody (1:1000) (Synaptic Systems) at 4ºC. Cells were washed five times with PBS, then incubated with Alexa Fluor 555-conjugated goat anti-rabbit secondary antibody (1:500) (Molecular Probes) at room temperature for 1h. After this, cells were washed five times with PBS and mounted on cover glasses with Fluoromont-G medium. Fluorescent images were randomly acquired using an inverted microscope (AxioVert 200, Zeiss). To visualize the iba–1 staining, microglia were excited by a xenon light source at 552 nm wavelength (exposure time, 0.8 s); in the case of beads, these were excited with a FITC-filter at 495 nm (exposure time, 0.8 s). The emission wavelengths were 578 and 519 nm, respectively. For the study of the effects of MCM and the rest of treatments on the number of phagocytosed beads (mean ± S. E. M.), bead-labelled cells were counted in four separate culturing procedures under the microscope with a 40x objective (blind analysis). Microglial cell area and intensity were measured from iba–1 cell fluorescence images through automatic thresholding selection (HCImage).

Statistical Analysis

Statistical analyses were carried out with the Mann-Whitney Rank Sum test (SPSS Statistics 25). All measurements were expressed as mean ± standard error of the mean (SEM), and $p \leq 0.05$ was considered significant.

Results

MCM triggers calcium transients essentially in resting microglia

In the present study, we stimulated cultured rat microglial cells with a pressure pulse (5 s) of MCM (Fig.1A). This cocktail of MCs mediators obtained by heat (53ºC, 1 h), showed a rapid and transient elevation of intracellular calcium ($[Ca^{2+}]_i$) in one out of two cells (167 out of 353 cells) measured by Fura–2 fluorescence (Fig. 1B, C). As MCs are temperature sensitive, the noxious physical stimuli (53 ºC) produced a clear degranulation verified by visual inspection under microscope (data not shown). This strategy elicits MC degranulation and avoids the use of stimuli such as compound 48/80, antigens, complement proteins or neuropeptides which can also activate microglia themselves. Interestingly, MCM obtained at 37 ºC, was also able to trigger intracellular Ca^{2+} elevation in 27% (6 out of 22) of microglial cells. At this temperature, MCs showed an intact appearance without clear degranulation. The increase in intracellular Ca^{2+} evoked in microglial cells by MCM at 37ºC was also transient and reached a peak of 0.23 ± 0.06 and area under curve (AUC) of 4.34 ± 1.12 that were similar to that induced by the MCM obtained by heat (53ºC) (F/F: 0.33 ± 0.01; AUC: 4.38 ± 0.24) (Fig. 1E, F).

Microglial cells with a ramified morphology with long, thin processes and small cell bodies are the major responders to the MCM (80.2 % at 53ºC and 100% at 37ºC) (Fig. 1G, H). These cells exhibit shapes typical of resting microglia and a weaker iba1 signal, a microglia-specific calcium-binding protein, in comparison with expression of iba1 in spindle, rod or amoeboid-shaped cells, corresponding to activated microglia (Fig. 1G). These data suggest that low secretion of mediators, such as the escape of biogenic amines from granules during basal activity of MCs (37ºC) is sufficient to evoke Ca^{2+} elevations mainly in those microglial cells with a resting phenotype.

Histamine is basically the mediator involved in microglia evoked Ca^{2+} transient

Next, we investigated which mediators were involved in this Ca^{2+} signaling. MCs contain a wide array of chemical mediators that can be released to the extracellular medium. We focused on the preformed products contained within the granules. To elucidate which mediators were involved in the promotion of microglia activation, we first directly stimulated microglial cells with bioactive monoamines (histamine, serotonin) and ATP. The effects of histamine (100 M) on Ca^{2+} signal in microglial cells were similar to those elicited by MCM 53ºC (Fig. 2A, B), with a 43% of response (83 out of 192 cells) (Fig. 2D) and, a $[Ca^{2+}]_i$ peak and area under curve of 99.1 ± 0.6% and 121.2 ± 10.5 %, respectively (Fig. 2E, F). Histamine mostly affected intracellular Ca^{2+} of resting cells (81.9% of cells) in consonance with the effects observed with MCM (80.2% of cells). However, serotonin did not evoke any response. On the contrary, external application of ATP (100 M) caused a Ca^{2+} transient (Fig. 2C) in most of the stimulated cells (94.8 %; 128 out of 135 cells) basically in activated microglia (70.9%) (Fig. 2D). In addition, while $[Ca^{2+}]_i$ peak was not different (88.6 ± 6 %) (Fig. 2E), the area under the curve was significantly lower (62.8 ± 3.1 %) (Fig. 2F) in ATP than in MCM-stimulated cells. When the selective antagonist of the histamine H1 receptor, cetirizine, was incubated within the cell chamber, 10 min before the application of histamine, Ca^{2+} transient response was completely abolished (Fig. 2B, D). Cetirizine also suppressed microglial activation induced by MCM, although a small pool of cells was resistant to the drug (10.3%; 21 out of 203 cells) (Fig. 2A, D). On the other hand, apyrase, an enzyme that catalyzes ATP hydrolysis, dramatically reduced ATP-response to 15.7 % (8 out of 51 cells); however, it did not affect MCM-microglia response (62.3%; 38 out of 61 cells) (Fig. 2A, C, D). Moreover, while $[Ca^{2+}]_i$ peak and the area under the curve were abruptly reduced in cells under ATP + Apyrase (F/F: 12.5 ± 4.1%: AUC: 4.3 ± 1.7%), the effect of apyrase on microglia response mediated by MCM was smaller. $[Ca^{2+}]_i$ peak was similar (107 ± 2.4 %), however, the area under the curve was lower (60.6 ± 10.7 %) than that obtained by application of MCM alone (Fig. 2E, F). Next, we selectively blocked PAR2 receptors with the antagonist FSLLRY-NH2 to determine the involvement of mast cell-specific proteases. We incubated cells for at least 10 min with FSLLRY-NH2 (400 M) before proceeding to apply MCM. The drug barely modified $[Ca^{2+}]_i$ signal evoked by MCM (F: 107.5 ± 10.2%; AUC: 105.7 ± 8.6%; 38 out of 70 cells)(Fig. 3B, E, F). Lastly, to resolve the implication of highly anionic serglycin proteoglycans (PGs) containing glycosaminoglycan side chains of either heparin

or chondroitin sulfate (CS) type in microglia activation, we incubated the MCM with heparinase or chondrotinase ABC for 1h at 37ºC to break down the PGs of heparin and CS, respectively. Chondroitinase ABC did not change the peak amplitude and the area under the curve of $[Ca^{2+}]_i$ transients in respect to untreated MCM (F: 95.6 ± 9.25%; area under curve: 99.9 ± 9.1%; 16 out of 30 cells) (Fig. 3C,E,F). Similarly, heparinase neither reduced the amount of $[Ca^{2+}]_i$ entry into the cell (F: 78.5 ± 7.7%; area under curve: 106 ± 9.1%; 32 out of 55 cells) (Fig. 3D, E, F). All these data suggest histamine H1 receptor mostly contributes to intracellular Ca^{2+} elevation in cultured microglia mediated by MCs. To a lesser extent, ATP also contributes in shaping the Ca^{2+} transient. Because histamine is the key mediator to initiate Ca^{2+} signaling that triggers microglia activation, we measured histamine concentration of used cocktails. On average, histamine concentration from MCM obtained at 53ºC (1 h) was 275 ± 90 M and at 37ºC (1h) of 17.5 ± 0.6 M.

Ca^{2+} dependent exocytosis in microglia stimulated by MCM and histamine

ATP is considered the major chemokine attracting microglia towards the injured brain regions [26] and microglia release ATP in response to stimuli which trigger intracellular calcium elevation [27]. Here, we incubated cells with quinacrine (10 μM for 10 min at room temperature), a fluorescent marker for intracellular ATP-enriched vesicles used to examine Ca^{2+} dependent regulated exocytosis of ATP [6][7]. We quantified exocytosis measuring fluorescence changes of cells after stimulation with MCM for 30s through a micro-perfusion pipette. As a control, application of an external solution produced a variable but gradual loss of fluorescence signal in 65% of cells which can be attributed to spontaneous vesicle fusion with the plasma membrane and dispersal of its fluorescent cargo (Fig. 4A, B, E). However, application of MCM induced a more abrupt loss of fluorescence (Fig. 4C, D, F) in 90,3% of cells to a significantly larger extent (F: 0.43 ± 0.02; n = 113) than that observed in control cells (F: 0.26 ± 0.04; n = 40). Furthermore, stimulation with histamine 100 M and LPS 1 g/ml also induced an important loss of fluorescence of 0.5 ± 0.04 and 0.49 ± 0.02, respectively, in more than 92% of cells (Fig. 4H). ATP did not increase significantly the exocytosis in 89.5% of cells affected by the nucleotide. Cells with an activated morphology prevail over those of resting phenotype when measuring exocytosis in all used treatments (Fig. 4G). These results suggest that despite few activated microglia were able to rise $[Ca^{2+}]_I$ in response to MCM, the vast majority of them undergo exocytosis of quinacrine loaded-organelles, comparable to that observed by histamine or LPS.

Divergent microglia metamorphosis induced by the MCM

As microglial activation is characterized by morphological changes and upregulation of the specific calcium-binding protein iba1, we analyzed the area and iba1-fluorescence in cells iba1-positive from control cells and cells treated during 6 h and 48 h with MCM 10%, histamine 10 and 100 M, ATP 100 M

and LPS 1 g/ml. MCM was diluted (1:10) because the pure extract (10^6 MCs/mL) would have required a wasteful volume of cells. Intriguingly, data analysis showed different results when using the two different cocktails of mediators assayed (named MCM1 and MCM2) so the results have been shown separately. Cells treated with histamine 100 M (HIS100) were not viable after 48 h of treatment and only 12 cells from 4 different cultures could be included in the analysis. MCM1 showed a reduction in area at 6 h (154 ± 10 m^2; n = 143) but an increase in area at 48 h (348 ± 20 m^2; n = 112) in respect to control cells (6h: 185 ± 9.5 m^2, n = 218; 48h: 194 ± 10 m^2, n = 238) (Fig. 5A, B, C). Nevertheless, MCM2 did not show differences in area at 6 h (201 ± 14 m^2; n = 125) or 48 h (200 ± 15 m^2; n = 133). Histamine 10 M (HIS10) showed an increase in area at 48 h (226 m ± 16 m^2; n = 251) while HIS100 reduced the area at 6 h (171 ± 8 m^2; n = 219) but it did not modify area at 48h (210 ± 41 m^2; n = 12). LPS showed an important increment of area at 6 h (293 ± 35 m^2; n = 166) and a reduction at 48 h (155 ± 9 m^2; n = 215) in respect to control cells. Finally, ATP only showed an increase of area in respect to control cells at 6 h (210 ± 9 m^2; n = 180) (Fig. 5A, B). On the other hand, the effects of both cocktails of mediators and both histamine concentrations did not change iba1 intensity at 6 h (Fig. 5D) but modified it significantly at 48h. MCM1 and HIS100 showed a similar tendency of reduction of iba1 fluorescence (MCM1: 26.1 ± 1.2; HIS100: 34.2 ± 2.3) in regard to control cells (49.6 ± 2.4) while MCM2 and HIS10, on the contrary, significantly raised iba1 intensity (MCM2: 56.6 ± 12.6; HIS10: 58.4 ± 2.3). The higher increment was obtained with LPS at 48 h (82.6 ± 3.5). ATP reduced iba1 intensity both at 6 h (48.8 ± 2.1) and 48 h (42.1 ± 1.7). Overall, MCM1 showed a similar pattern of area modification and Iba1 expression to histamine 100 M while MCM2 showed a similar response to histamine 10 M. The concentration of histamine was measured and resulted in 21 µM for the MCM1 and 3.7 µM for the MCM2. These results indicate that the histamine concentration regulated the level of iba1 expression, hence it could derive in two opposite microglia phenotypes, which was confirmed when phagocytosis was studied.

The phagocytotic phenotype of microglia is determined by the histamine concentration in the MCM

Phagocytosis was assessed by using fluorescent latex beads of 1m under the same conditions and incubation intervals as above. Both MCM1 and HIS100 showed a reduction in the engulfment of microspheres per cell at 6h (MCM1: 0.71 ± 0.1; HIS100: 1.1 ± 0.1) and 48h (MCM1: 0.66 ± 0.17; HIS100: 0.33 ± 0.22) regarding control cells (6h:1.5 ± 0.2; 48h:1.92 ± 0.2) (Fig. 6A, B). MCM2 and HIS10 also showed a similar value of uptake of fluorescent beads. Neither of them affected phagocytosis at 6 h yet increased the internalization of microspheres at 48h (MCM2: 3.07 ± 0.35; HIS10: 3.08 ± 0,2) to the same extent as LPS (2.91 ± 0.3). ATP did not modify phagocytosis at any time (1.8 ± 0.2, 6h; 1.94 ± 0.2, 48h). A clear concordance was again observed in the responses between MCM1 and HIS100 and between MCM2 and HIS10. In addition, once more, inverse effects on phagocytosis were observed between the two assayed cocktails with low and high concentrations of histamine. The percentage of total cells with phagocytosed beads was 49.8 % (6h) and 51.3% (48h) in control cells. Among these, a small number of cells were able to uptake more than 6 beads (7.3%, 6h; 10.1%, 48h). This number was almost non-existent

in cells treated with MCM1 (0 %, 6h; 2.7%, 48h) and HIS100 (5%, 6h; 0%, 48h), but it increased in cells treated with MCM2 (6.4%, 6h; 18.1%, 48h) and HIS10 (7.7%, 6h; 20.3%, 48h) for 48 h (Fig. 6D, E). LPS was a positive activator of phagocytosis (12.1%, 6h; 20%, 48h) while ATP had a behavior similar to control cells (11.7%, 6h; 11%, 48h).

Finally, in order to understand how morphological changes and iba1-intensity can influence functional responses of microglia, we have related these two parameters with phagocytosed beads per cell. Interestingly, we observed an exponential relationship between the area and engulfed beads at 6 h. In short periods, larger cells are more active in phagocytosis (Fig. 6F). This relation was not observed at 48 h (Fig. 6G, inset). In contrast, iba1 expression was a better value to predict phagocytosis at longer times. There is a sigmoidal relation between iba1 intensity and the number of beads per cell in each condition at 48 h (Fig. 6G). Higher fluorescence intensity indicates higher intakes of beads. This relationship could not be observed at 6 h (Fig. 6F, inset).

Discussion

In basal conditions, MCs can undergo spontaneous exocytosis that results in secretion of histamine. Extracellular medium from resting MCs (10^6/ml) kept for 1h at 37ºC showed a histamine concentration of 17 M, a dose high enough to increase intracellular [Ca^{2+}] of ramified microglia (Fig.1D). At 53ºC, MCs showed a degranulated phenotype, suggesting a stronger and complete degranulation able to increase histamine concentration to ≈275 M (on average). Curiously, in terms of Ca^{2+} signal, there were no differences in Ca^{2+} peak and the area under the curve of microglial cells activated by MCM at 37 ºC or 53ºC, although a higher number of cells were affected at 53ºC (Fig. 1E, F). This activation in microglia is principally mediated by H1 receptor (H1R) since, after the blockade of H1R by cetirizine, the Ca^{2+} signal evoked by histamine 100 M was completely inhibited. To a much lesser extent, ATP seems to contribute to create the Ca^2 signal (Fig. 2C, F).

As ATP-exocytosis is triggered by an elevation of $[Ca^{2+}]_i$, we characterized Ca^{2+} dependent exocytosis in microglia by loading the cells with quinacrine. Although the increase in $[Ca^{2+}]_i$ induced by MCM was mainly observed in resting microglia, we found a loss of quinacrine fluorescence mostly in activated cells. Microglia isolated from mixed cultures by mild trypsinization, as we performed, it is considered to show uniform ramified morphology unlike the more heterogeneous microglia isolated by using the shaking method [24]. Nevertheless, our cultures showed a certain level of activation and this activation at baseline may likely increase basal $[Ca^{2+}]_i$ and affect the exocytotic response in stimulated and non-stimulated cells. Anyway, in response to MCM and histamine, microglia exhibited a higher exocytotic response than the one measured in control cells. Since lysosomal exocytosis has been suggested to be involved in cytokine release in monocytes and microglia [8][9], it is likely that microglial exocytosis is at least partly responsible for the release of pro-inflammatory factors tumor necrosis factor (TNF)-alpha and interleukine–6 (IL–6) from microglia stimulated with MC mediators [17]. Histamine, is a MC mediator which can stimulate microglia activation in a dose-dependent manner and subsequently, production of

TNF-α and IL–6 [28]. The release of such mediators has been shown to be suppressed by H1R and H4R antagonists [28][17]. This insight may partly confirm the abolishment of $[Ca^{2+}]_i$ signal by the H1R antagonist cetirizine and suggests that TNF-α and IL–6 may be released by a Ca^{2+} dependent exocytosis.

Iba1 is a calcium-binding protein which is expressed specifically in microglia [29] and is upregulated in activated cells [30]. This is a cytoplasmic helix-loop-helix protein with F-actin binding and actin-cross-linking activity, possibly involved in cell motility and phagocytosis [30][31][32]. Our experiments confirm the role of iba1 in phagocytosis of longer activated microglia, given the relationship between iba1 intensity and phagocytosed microbeads (Fig. 6G). While LPS, histamine 10 μM and MCM2 ([His] = 3.7 μM) increased iba1 fluorescence and engulfed beads at 48h, histamine 100 μM and MCM1 ([His] = 21μM) had the opposite effect, reducing iba1 signal and concomitantly, the phagocytic activity (Fig. 5E & 6C). When cells were treated for a shorter period (6h), phagocytosis was not dependent on iba1 expression but instead showed a correlation with cell area. The greater the cell size, the higher the chance of phagocytosis. The net area should be the result between the exocytotic and endocytic cell balance. However, microglia also utilizes several non-vesicular mechanisms of secretion (exosomes and ectosomes) that may be altered in relation to the activation state of microglia [21]. LPS showed the larger increased area at 6 h (Fig. 5B). Interestingly, MCM1 and high histamine reduced the cell area (Fig. 5B) despite the lesser membrane internalization by phagocytosis (Fig. 6B, C) and the intense exocytosis (Fig. 4H), suggesting participation of non-vesicular mechanisms. Histamine 100 μM and MCM1 reduced the number of cells with beads quickly and this inhibitory effect was accentuated in cells after 48 h of incubation, while low histamine and MCM2-treated cells behaved as control cells with no changes in phagocytosis (Fig. 6B), until the iba1 expression was increased. Otherwise, despite MC-derived ATP appears to participate in microglia $[Ca^{2+}]_i$ elevation, it does not seem to be involved in morphological changes, iba–1 expression and phagocytotic modifications mediated by the MCM at low and high histamine concentrations.

Histamine has been previously probed to promote microglial phagocytosis via H1R [33] and the response was dose dependent (range from 1 to 100 μM). Histamine binding to the H1R triggers G-protein alpha q–11 (Gαq) activation with the subsequent stimulation of phospholipase C (PLC) that leads to the generation of inositol phosphates (IP3) and diacylglycerol (DAG) [34]. The functional coupling of the H1R to Gαq-PLC leads to the activation of the Rac small GTPase [35], and Rac is considered a key molecule in microglia activation which regulates reorganization of the actin cytoskeleton [29]. Furthermore, iba1 also enhances Rac activation, via a PLCβ dependent pathway [36]. On the other hand, an inhibition of microglial phagocytosis was also reported through H3R at concentrations above 10 μM of histamine [37]. Despite contradictory data in relation to the concentrations required to promote or inhibit phagocytic activity in microglia (which may be due to the different types of cells used and experimental protocols), our results reveal a dual role of histamine; evidence that, by the way, has already been described on microglia-induced neurodegeneration [38][39]. Low levels of histamine, such as those expected to exist in the surroundings of resting brain MCs can increase $[Ca^{2+}]_i$, iba1 expression and phagocytosis of nearby microglia, which may be beneficial to inhibit acute insults. However, strong or chronic brain MCs

stimulation can augment histamine concentration and promote the opposite effect on microglia phagocytosis. In this scenario, a neurotoxic instead of neuroprotective microglia phenotype may be expected.

The role of MCs in determining the microglial phenotype in Alzheimer and other pathologies can be crucial [40][41]. MCs are among the first brain cells to sense amyloid beta peptides [42] and MCs treated with A enhanced histamine release [43] that, according to our data, could decide the microglial phagocytotic response. Features of microglia that relate to phagocytosis are beneficial in Alzheimer's disease by degrading A plaques [44]. Therefore, the inhibition of MC degranulation could be a useful therapeutic strategy to limit brain histamine concentration and, as a result, reduce proinflammatory cytokines (TNF-alpha, IL–6) and increase A phagocytosis by microglia. Besides, a delicate regulation of the microglial phagocytosis seems to be critical in Parkinson disease, multiple sclerosis and other brain diseases [45][46][47].

We have recently demonstrated a bidirectional communication between MCs and hippocampal neurons [22]. Proteoglycans of CS released from MCs granules are involved in neuronal activation and $[Ca^{2+}]_i$ elevation. Exocytosis is a delicate regulated process. While exocytosis through the kiss-and-run (reversible fusion) mechanism promotes a small release of soluble mediators such as histamine and serotonin [48][49], full fusion or complete granule fusion allows the extrusion of proteoglycans matrix and proteins, mediators of high molecular weight, which require the complete expansion of the exocytotic fusion pore to exit [50]. Therefore, while an acute stimulation of MCs can allow a rapid release of a small amount of histamine through kiss-and-run, the intense and continuous MC activation would produce degranulation with massive histamine and proteoglycans extrusion [51] which can compromise microglial phagocytic clearance function and activate hippocampal neurons, and therefore contributing to increase neuronal $[Ca^{2+}]_i$ overload and unwanted material among the CNS environment. Since the elimination of unwanted and potentially harmful matter is crucial for CNS function, regulation of microglia phagocytosis by MCs may have a key role in neuroinflammation.

Conclusions

MCs-derived histamine is a key molecule in the modulation of microglia phagocytosis which is crucial for CNS homeostasis. MCs are resident cells of the brain and one of the most important sources of histamine during systemic inflammation so that the control of degranulation by MCs stabilizers in combination with histamine receptors antagonists may be a valuable therapeutic approach in neuroinflammatory disorders.

References

1. Kovacs GG. Concepts and classification of neurodegenerative diseases. Handb Clin Neurol. Elsevier B. V.; 2017. p. 301–7.

2. Dugger BN, Dickson DW. Pathology of Neurodegenerative Diseases. Cold Spring Harb Perspect Biol. 2017;9:7.
3. Kettenmann H, Hanisch U-K, Noda M, Verkhratsky A. Physiology of microglia_ sup info. Physiol Rev. 2011; 91:461–553.
4. Hanisch UK, Kettenmann H. Microglia: Active sensor and versatile effector cells in the normal and pathologic brain. Nat. Neurosci. 2007. p.1387–94.
5. Sharma P, Ping L. Calcium ion influx in microglial cells: physiological and therapeutic significance. J Neurosci Res. 2014;92:409–23.
6. Dou Y, Wu HJ, Li HQ, Qin S, Wang YE, Li J, et al. Microglial migration mediated by ATP-induced ATP release from lysosomes. Cell Res. 2012;22:1022–33.
7. Imura Y, Morizawa Y, Komatsu R, Shibata K, Shinozaki Y, Kasai H, et al. Microglia release ATP by exocytosis. Glia. 2013;61:1320–30.
8. Andrei C, Margiocco P, Poggi A, Lotti L V, Torrisi MR, Rubartelli A. Phospholipases C and A2 control lysosome-mediated IL–1 beta secretion: Implications for inflammatory processes. Proc Natl Acad Sci U S A. 2004;101:9745–50.
9. Eder C. Mechanisms of interleukin–1β release. Immunobiology. 2009. p. 543–53.
10. Greenberg S, el Khoury J, di Virgilio F, Kaplan EM, Silverstein SC. Ca(2+)-independent F-actin assembly and disassembly during Fc receptor-mediated phagocytosis in mouse macrophages. J Cell Biol. 1991;113:757–67.
11. Kalla R, Bohatschek M, Kloss CUA, Krol J, Von Maltzan X, Raivich G. Loss of microglial ramification in microglia-astrocyte cocultures: involvement of adenylate cyclase, calcium, phosphatase, and Gi-protein systems. Glia. 2003;41:50–63.
12. Silver R, Curley JP. Mast cells on the mind: new insights and opportunities. Trends Neurosci. 2013;36:513–21.
13. Silverman AJ, Sutherland AK, Wilhelm M, Silver R. Mast cells migrate from blood to brain. J Neurosci. 2000;20:401–8.
14. Wernersson S, Pejler G. Mast cell secretory granules: Armed for battle. Nat. Rev. Immunol. Nature Publishing Group; 2014. p. 478–94.
15. Galli SJ, Nakae S, Tsai M. Mast cells in the development of adaptive immune responses. Nat Immunol. 2005;6:135–42.
16. Zhang S, Zeng X, Yang H, Hu G, He S. Mast cell tryptase induces microglia activation via protease-activated receptor 2 signaling. Cell Physiol Biochem. 2012;29:931–40.
17. Zhang X, Wang Y, Dong H, Xu Y, Zhang S. Induction of Microglial Activation by Mediators Released from Mast Cells. Cell Physiol Biochem. 2016;38:1520–31.
18. Dong H, Zhang X, Wang Y, Zhou X, Qian Y, Zhang S. Suppression of Brain Mast Cells Degranulation Inhibits Microglial Activation and Central Nervous System Inflammation. Mol Neurobiol. 2017;54:997–1007.

19. Dong H, Wang Y, Zhang X, Zhang X, Qian Y, Ding H, et al. Stabilization of Brain Mast Cells Alleviates LPS-Induced Neuroinflammation by Inhibiting Microglia Activation. Front Cell Neurosci. 2019;13:191.
20. Zhang X, Dong H, Li N, Zhang S, Sun J, Zhang S, et al. Activated brain mast cells contribute to postoperative cognitive dysfunction by evoking microglia activation and neuronal apoptosis. J Neuroinflammation. 2016;13:127.
21. Prada I, Furlan R, Matteoli M, Verderio C. Classical and unconventional pathways of vesicular release in microglia. Glia. 2013;61:1003–17.
22. Flores JA, Ramírez-Ponce MP, Montes MÁ, Balseiro-Gómez S, Acosta J, Álvarez de Toledo G, et al. Proteoglycans involved in bidirectional communication between mast cells and hippocampal neurons. J Neuroinflammation. 2019;16:107.
23. Parada E, Egea J, Buendia I, Negredo P, Cunha AC, Cardoso S, et al. The microglial α7-acetylcholine nicotinic receptor is a key element in promoting neuroprotection by inducing heme oxygenase–1 via nuclear factor erythroid–2-related factor 2. Antioxid Redox Signal. 2013;19:1135–48.
24. Lin L, Desai R, Wang X, Lo EH, Xing C. Characteristics of primary rat microglia isolated from mixed cultures using two different methods. J Neuroinflammation. 2017;14:101.
25. Lian H, Roy E, Zheng H. Microglial Phagocytosis Assay. BIO-PROTOCOL. Bio-Protocol, LLC; 2016;6.
26. Davalos D, Grutzendler J, Yang G, Kim J V, Zuo Y, Jung S, et al. ATP mediates rapid microglial response to local brain injury in vivo. Nat Neurosci. 2005;8:752–8.
27. Liu GJ, Kalous A, Werry EL, Bennett MR. Purine release from spinal cord microglia after elevation of calcium by glutamate. Mol Pharmacol. 2006;70:851–9.
28. Dong H, Zhang W, Zeng X, Hu G, Zhang H, He S, et al. Histamine induces upregulated expression of histamine receptors and increases release of inflammatory mediators from microglia. Mol Neurobiol. 2014;49:1487–500.
29. Imai Y, Kohsaka S. Intracellular Signaling in M-CSF-Induced Microglia Activation: Role of Iba1. Glia. 2002;40:164–74.
30. Ito D, Tanaka K, Suzuki S, Dembo T, Fukuuchi Y. Enhanced expression of Iba1, ionized calcium-binding adapter molecule 1, after transient focal cerebral ischemia in rat brain. Stroke. Lippincott Williams and Wilkins; 2001;32:1208–15.
31. Ito D, Imai Y, Ohsawa K, Nakajima K, Fukuuchi Y, Kohsaka S. Microglia-specific localisation of a novel calcium binding protein, Iba1. Mol Brain Res. 1998;57:1–9.
32. Sasaki Y, Ohsawa K, Kanazawa H, Kohsaka S, Imai Y. Iba1 is an actin-cross-linking protein in macrophages/microglia. Biochem Biophys Res Commun. Academic Press Inc.; 2001;286:292–7.
33. Rocha SM, Saraiva T, Cristóvão AC, Ferreira R, Santos T, Esteves M, et al. Histamine induces microglia activation and dopaminergic neuronal toxicity via H1 receptor activation. J Neuroinflammation. 2016;13:137.
34. Hill SJ, Ganellin CR, Timmerman H, Schwartz JC, Shankley NP, Young JM, et al. International union of pharmacology. XIII. Classification of histamine receptors. Pharmacol. Rev. 1997. p. 253–78.

35. Notcovich C, Diez F, Tubio MR, Baldi A, Kazanietz MG, Davio C, et al. Histamine acting on H1 receptor promotes inhibition of proliferation via PLC, RAC, and JNK-dependent pathways. Exp Cell Res. Academic Press Inc.; 2010;316:401–11.
36. Kanazawa H, Ohsawa K, Sasaki Y, Kohsaka S, Imai Y. Macrophage/microglia-specific protein Iba1 enhances membrane ruffling and Rac activation via phospholipase C-gamma -dependent pathway. J Biol Chem. 2002;277:20026–32.
37. Iida T, Yoshikawa T, Matsuzawa T, Naganuma F, Nakamura T, Miura Y, et al. Histamine H3 receptor in primary mouse microglia inhibits chemotaxis, phagocytosis, and cytokine secretion. Glia. 2015;63:1213–25.
38. Barata-Antunes S, Cristóvão AC, Pires J, Rocha SM, Bernardino L. Dual role of histamine on microglia-induced neurodegeneration. Biochim. Biophys. Acta - Mol. Basis Dis. Elsevier B. V.; 2017. p. 764–9.
39. Ferreira R, Santos T, Gonçalves J, Baltazar G, Ferreira L, Agasse F, et al. Histamine modulates microglia function. J Neuroinflammation. 2012;9.
40. Kempuraj D, Selvakumar GP, Thangavel R, Ahmed ME, Zaheer S, Raikwar SP, et al. Mast Cell Activation in Brain Injury, Stress, and Post-traumatic Stress Disorder and Alzheimer's Disease Pathogenesis. Front Neurosci. 2017;11:703.
41. Hendriksen E, van Bergeijk D, Oosting RS, Redegeld FA. Mast cells in neuroinflammation and brain disorders. Neurosci Biobehav Rev. Pergamon; 2017;79:119–33.
42. Niederhoffer N, Levy R, Sick E, Andre P, Coupin G, Lombard Y, et al. Amyloid β Peptides Trigger CD47-Dependent Mast Cell Secretory and Phagocytic Responses. Int J Immunopathol Pharmacol. SAGE PublicationsSage UK: London, England; 2009;22:473–83.
43. Harcha PA, Vargas A, Yi C, Koulakoff AA, Giaume C, Sáez JC. Hemichannels are required for amyloid β-Peptide-induced degranulation and are activated in brain mast cells of APPswe/PS1dE9 Mice. J Neurosci. Society for Neuroscience; 2015;35:9526–38.
44. Majumdar A, Cruz D, Asamoah N, Buxbaum A, Sohar I, Lobel P, et al. Activation of microglia acidifies lysosomes and leads to degradation of Alzheimer amyloid fibrils. Mol Biol Cell. 2007;18:1490–6.
45. Fu R, Shen Q, Xu P, Luo JJ, Tang Y. Phagocytosis of microglia in the central nervous system diseases. Mol Neurobiol. 2014;49:1422–34.
46. Tremblay M-E, Cookson MR, Civiero L. Glial phagocytic clearance in Parkinson's disease. Mol Neurodegener. 2019;14:16.
47. Hanisch U-K, Kettenmann H. Microglia: active sensor and versatile effector cells in the normal and pathologic brain. Nat Neurosci. 2007;10:1387–94.
48. de Toledo GA, Fernández-Chacón R, Fernández JM. Release of secretory products during transient vesicle fusion. Nature. Nature Publishing Group; 1993;363:554–8.
49. Fernández-Peruchena C, Navas S, Montes MA, Alvarez de Toledo G. Fusion pore regulation of transmitter release. Brain Res Brain Res Rev. 2005;49:406–15.

50. Fulop T, Smith C. Physiological stimulation regulates the exocytic mode through calcium activation of protein kinase C in mouse chromaffin cells. Biochem J. 2006;399:111–9.
51. Flores JA, Balseiro-Gómez S, Ales E. Emerging Roles of Granule Recycling in Mast Cell Plasticity and Homeostasis. Crit Rev Immunol. 2016;36:461–84.

List Of Abbreviations

MC: Mast cell, MCM: cocktail of MC mediators; $[Ca^{2+}]_i$:intracellular calcium concentration, PG: proteoglycans, CS: chondroitin sulfate, LPS: lipopolysaccharide, CNS: Central Nervous System.

Declarations

Ethics approval

The experiments carried out in this work have been approved by the Ethics Committees of Seville University School of Medicine and the Consejeria de Agricultura, Pesca y Desarrollo Rural de la Junta de Andalucía, Spain

Consent for publication

Not applicable.

Availability of data and material

All data are available upon request.

Competing interests

The authors declare that they have no competing interests

Funding

This work was supported by grant from the Spanish Ministry of Economy and Competitivity (BFU2017–85832R), co-funded by the European Social Fund and the Junta de Andalucía (BIO–236).

Authors’ contributions

JAFC, ASG, SBG, MDM and JA carried out all the experiments and data analysis. JAFC, PRP and EA designed experiments, analyzed and discussed results, and wrote the paper. All authors have read and

approved the final manuscript

Authors' information

Present address for Santiago Balseiro Gomez: Department of Neuroscience, Yale School of Medicine, 295 Congress Avenue, New Haven, CT 06510, USAEmail address: santiago.balseirogomez@yale.edu

Acknowledgements

We thank Dolores Gutierrez and Laura Sánchez for their technical support.

Figures

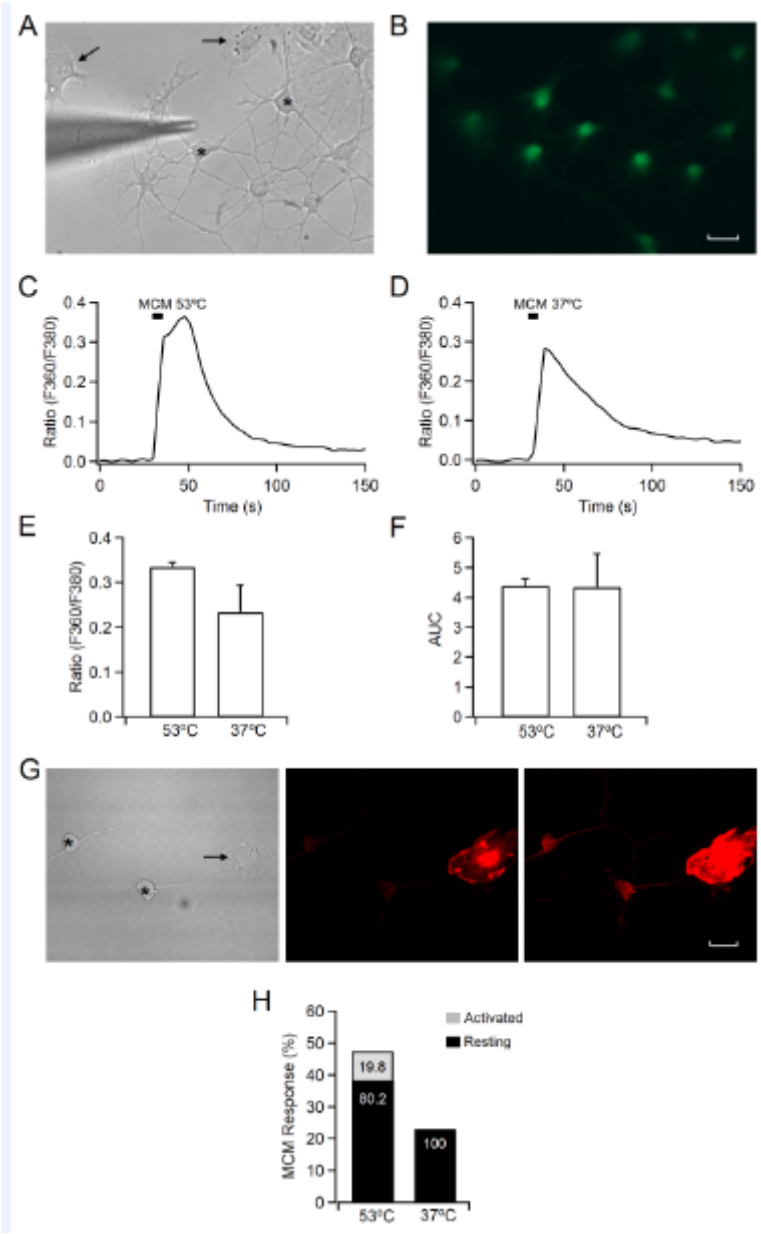

Figure 1

Calcium imaging of microglial cells. A) Phase-contrast image of rat cultured microglia and a glass micropipette of 1□m □ connected to a picospritzer which applies 5 s pressure ejection (2.5 psi) pulses. B) Fluorescence image showing the same cells loaded with the Ca2+ sensitive dye Fura 2-AM. C) Representative trace of [Ca2+]i transient in a cell evoked by the application of MCM obtained after MCs degranulation at 53ºC. D) Representative trace of [Ca2+]i transient in a cell evoked by application of MCM obtained after MCs incubation at 37ºC. E) Mean [Ca2+]i peak and F) Area under curve (AUC) obtained in microglia-evoked responses by stimulation with MCM at 53 ºC and 37ºC. G) Anti-Iba1 immunostaining of microglial cells with different morphological phenotype (2 resting cells with ramified long processes and rounded cell bodies (*) and 1 activated cell with an amoeboid appearance (arrow)). Left panel shows cells in bright-field, middle and right panels show fluorescence images taken at 60X and a 366 hV and 536 hV of gain, respectively. H) Percentage of microglia activated by MCM at 53ºC and 37ºC. Numbers inside the bars indicate the proportion of activated or resting cells that showed a [Ca2+]i transient after MCM application. Scale bar: 10 □m

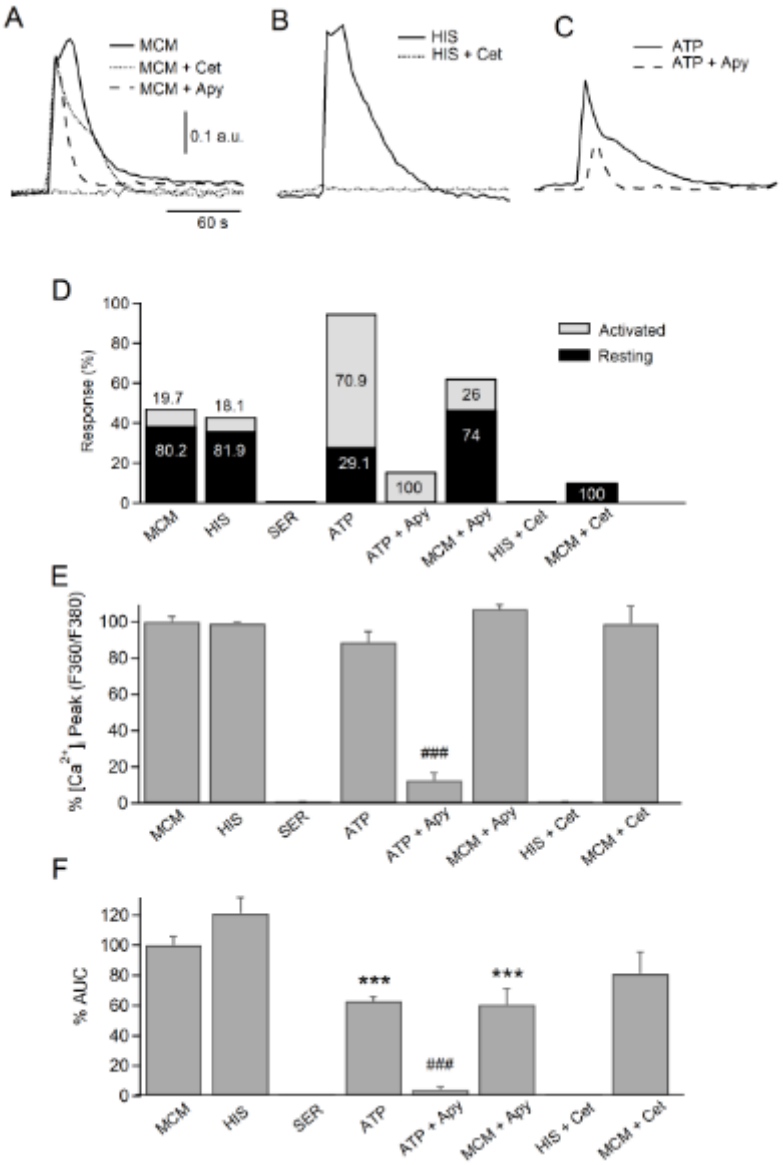

Figure 2

Histamine and ATP contribute to outline the [Ca2+]i signal elicited by mast cells mediator cocktail. A) [Ca2+]i signals evoked by single 5 s pressure ejection pulses of MCM alone (solid trace) and MCM applied after cetirizine (Cet) 1 □M (dotted line) and apyrase (Apy) 50 U/ml (dashed line) treatment (10 min). B) Representative [Ca2+]i signals evoked by histamine (HIS) 100 □M (solid line) and histamine 100 □M applied after cetirizine 1 □M (dotted line) treatment (10 min). C) Representative [Ca2+]i signals evoked by single pressure pulses of ATP 100 □M (solid line) and ATP 100 □M (dashed line) applied after apyrase 50 U/ml treatment (10 min). D) Percentage of cells which displayed [Ca2+]i transients in response to the different treatments according to the observed phenotype. Numbers inside the bars designate the proportion of activated or resting microglia in respect to the total cells that responded. E) [Ca2+]i signal amplitude (peak) and F) area under curve (AUC) obtained by application of MCM, histamine 100, histamine following incubation with cetirizine (HIS + Cet), serotonin (SER), ATP, ATP after incubation with apyrase (ATP + Apy), MCM after incubation with cetirizine (MCM + Cet) and MCM after incubation with apyrase (MCM + Apy) are presented as % of means ± SEM. Data were normalized regarding the MCM response. ### Statistically significant from MCM-treated cells ($p<0.001$), ***Statistically significant from ATP-treated cells ($p<0.001$).

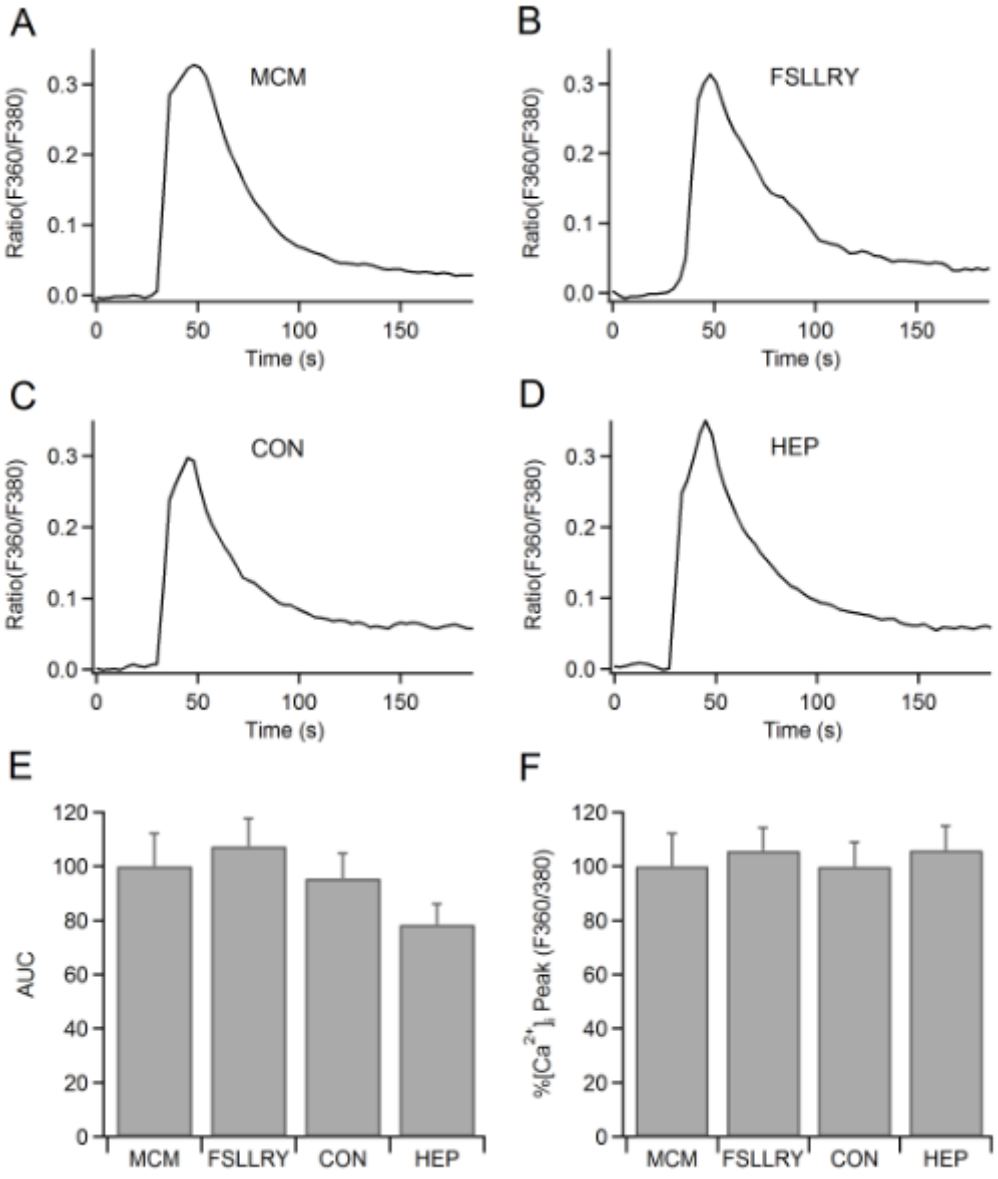

Figure 3

PGs of CS and heparin did not contribute to outline the [Ca2+]i signal elicited by mast cells mediator cocktail. A) Trace illustrating a control MCM-evoked response. B) The response did not change after incubation with FSLLRY-NH2. C) Neither pre-digestion of MCM with chondroitinase ABC nor D) heparinase modified [Ca2+]i transients. E) [Ca2+]i signal amplitude (peak) and F) area under curve (AUC) are presented as % of means ± SEM.

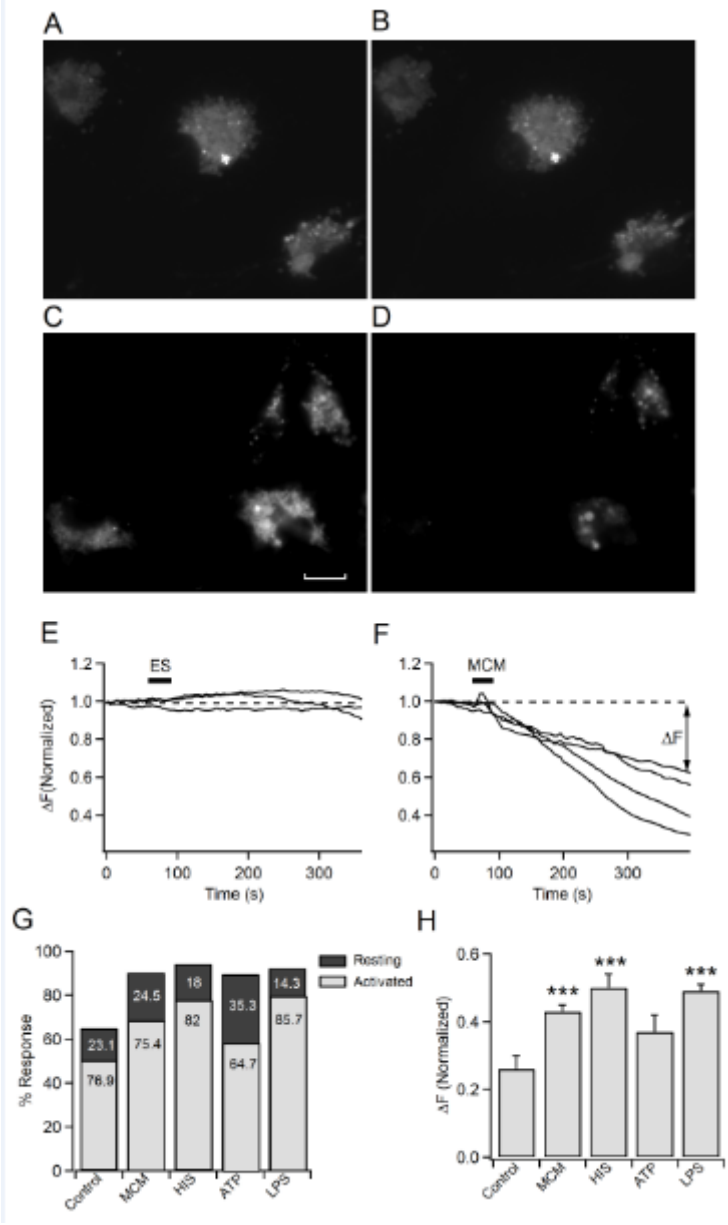

Figure 4

Changes in fluorescence intensity of quinacrine-loaded cells during exocytosis. A) Example image of quinacrine loaded microglia cells before and B) ≈5 min after application of external solution by micro-perfusion (control experiment). C) Example image of quinacrine loaded microglia cells before and D) ≈5 min after application of MCM. A larger loss of fluorescence was observed in respect to control. E) Time courses of fluorescence changes (normalized) in control cells and F) MCM treated cells from the upper images. G) Percentage of microglial cells (resting versus activated) that showed a positive exocytotic response (fluorescence decay >5% FINITIAL) following stimulation with MCM, histamine (HIS), ATP, and LPS. Numbers inside the bars designate the proportion of activated or resting microglia that showed an exocytotic response under the indicated treatments. H) Amplitude (ΔF) measured from fluorescence curves (FINITIAL – FFINAL). Data represent average values of at least three independent culturing experiments. Scale bar 5 μm. ***p<0.001.

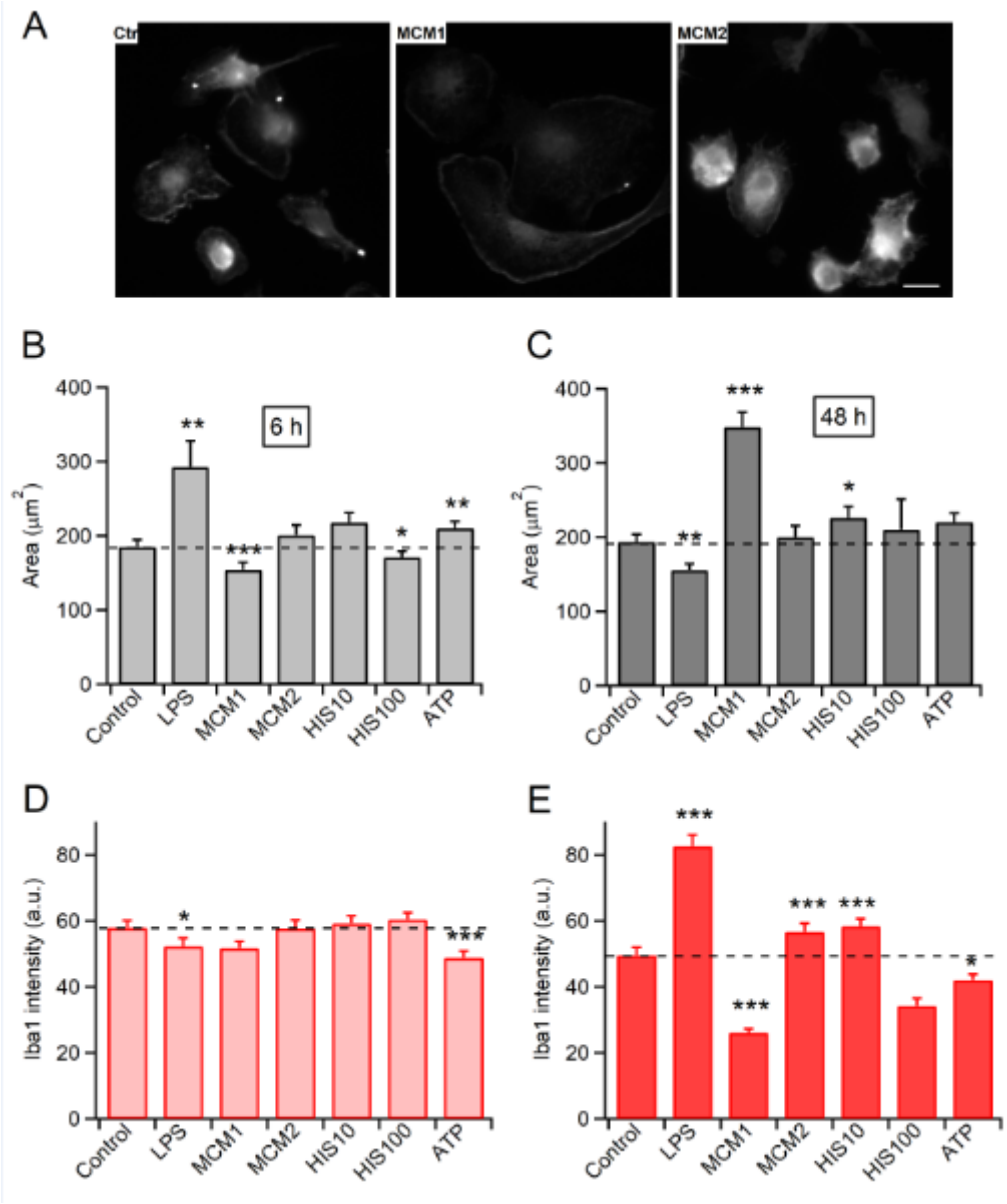

Figure 5

MCM activates two different morphological changes and iba1 expression in microglia determined by the histamine concentration. A) Representative images of iba1-positive microglia cells in non-treated cells (left panel) and treated with MCM1 ([His] = 21 μM) (middle panel), and MCM2 ([His] = 3.7 μM) (right panel). B) Surface area of cells treated for 6 h and C) 48 h with MCM1, MCM2, histamine 10 μM (HIS10), histamine 100 μM (HIS100), ATP 100 μM and LPS 1 μg/ml. D) Iba1 fluorescence intensity in cells treated for 6 h and E) 48 h with MCM1, MCM2, HIS10, HIS100, ATP 100 μM and LPS 1 μg/ml. Values (mean ± S.E.M) were computed from four independent culturing experiments. *p< 0.05; ***p<0.001. Scale bar 5 μm.

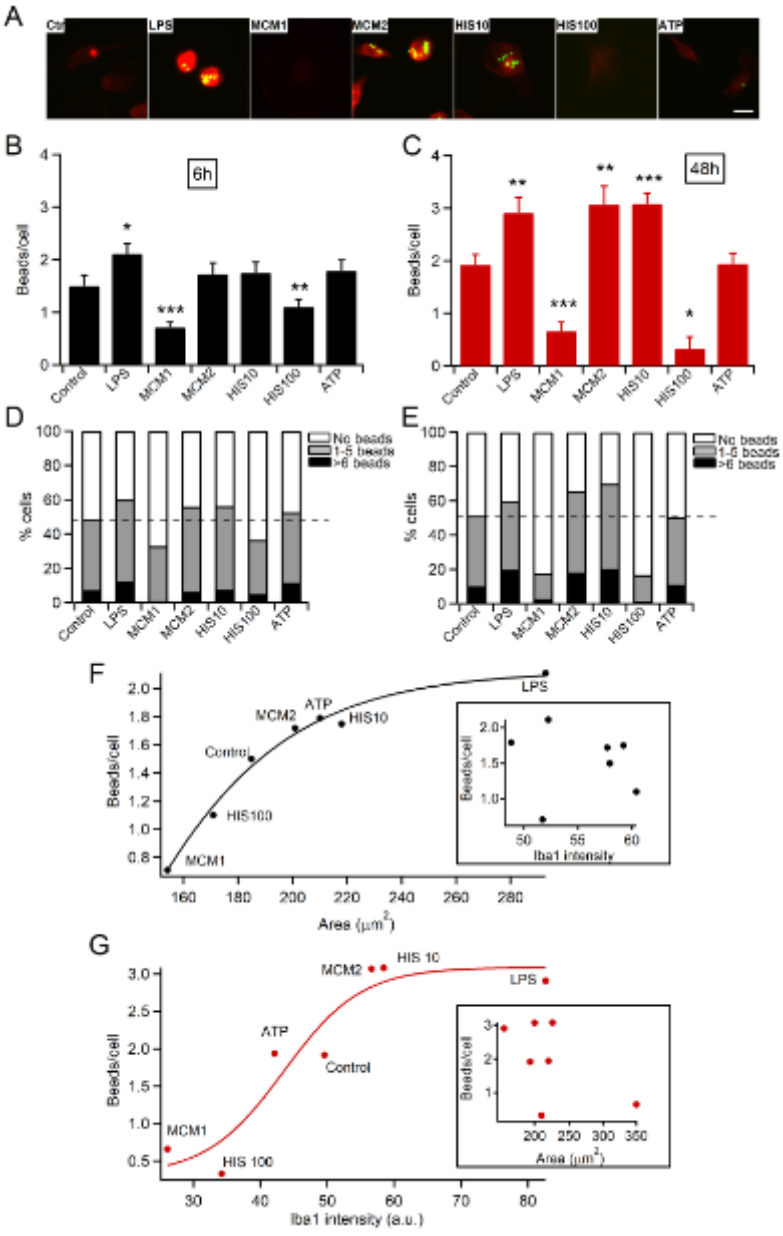

Figure 6

MCM activates two facing phagocytic phenotypes in microglia determined by the histamine concentration. A) Representative images illustrate latex microbeads phagocytosis of iba1-positive (red) microglial cells in non-treated cells (Ctr) and treated cells with LPS, MCM1 ([His] = 21 μM), MCM2 ([His] = 3.7 μM), histamine 10 μM (HIS10), histamine 100 μM (HIS100) and ATP 100 μM. B) Only LPS significantly increased the number of phagocytosed beads per cell compared with controls at 6 h. MCM1 and HIS100 even diminished phagocytosed beads regarding untreated cells. C) Potentiation of phagocytosis by LPS, MCM2 and HIS100 at 48 h. The inverse effect is induced by MCM1 and HIS100. D) Percentage of cells treated for 6 h and E) 48 h without beads (white bar), between 1-5 beads (grey bar) and more than 6 beads (black bar). F) Exponential relation between area and beads per cell at 6 h. Inset includes graph showing there is no relation between iba1 intensity and beads per cell at 6 h. G) Sigmoidal relation between iba1 intensity and beads per cell at 48 h. Inset includes graph showing there is no

relation between area and beads per cell at 48 h. Values (mean ± S.E.M) were computed from four independent culturing experiments. *p< 0.05; ***p<0.001. Scale bar 5 μm.